Defense Technical Information Center Compilation Part Notice

ADP013657

TITLE: A Comparison of Adaptive Mesh Refinement Approaches for Large Eddy Simulation

DISTRIBUTION: Approved for public release, distribution unlimited

This paper is part of the following report:

TITLE: DNS/LES Progress and Challenges. Proceedings of the Third AFOSR International Conference on DNS/LES

To order the complete compilation report, use: ADA412801

The component part is provided here to allow users access to individually authored sections of proceedings, annals, symposia, etc. However, the component should be considered within the context of the overall compilation report and not as a stand-alone technical report.

The following component part numbers comprise the compilation report:
ADP013620 thru ADP013707

A COMPARISON OF ADAPTIVE MESH REFINEMENT APPROACHES FOR LARGE EDDY SIMULATION

Sorin M. Mitran

Department of Applied Mathematics
University of Washington
Box 352420, Seattle, WA, 98195-2420, USA
mitran@amath.washington.edu

Abstract   A number of approaches to the problem of using adaptive mesh refinement in large eddy simulations are considered and tested. These include unstructured and structured adaptive grids, various treatments of the convective terms and a number of flow diagnostic procedures. The approaches are exemplified on a rotating channel flow.

Introduction

An important aspect in applying large eddy simulation (LES) to technologically interesting flows is the control of the computational costs involved. Complex flows usually present a variety of regions in which different resolutions are called for. Moreover, these regions are not static in the course of the flow evolution. Adaptive mesh refinement is a natural candidate for keeping computational costs down in these types of applications. In this paper a number of approaches are compared in an effort to provide information on the benefits of applying adaptive mesh refinement techniques to LES computations. A first comparison is made between an unstructured grid algorithm and a structured grid algorithm. The same computational procedures are implemented in both codes and comparable resolutions are achieved on a moderately complex flow. The results are compared to one another and a direct numerical simulation (DNS) to permit evaluation of grid quality effects. An additional comparison is made between various criteria of controlling the mesh adaptation. A variety of flow feature diagnostic procedures are allowed to control placement of additional grid points. These include

comparison to predictor steps on coarser grids and refinement according to local values of vorticity.

1.   Adaptive Mesh Refinement for LES

1.1   General observations

Adaptive mesh refinement (AMR) [5] has shown itself to be a powerful technique in the computation of flows with dynamic localized structures that require much greater resolution than that needed for most areas of the flow. AMR has been widely applied to flows involving shocks or chemical reactions. There has been less work in the area of applying AMR to turbulent flow. AMR is not suitable for turbulent flows in which fine resolution is required everywhere. There are however a number of flows in which small-scale structures appear and then drive the overall flow. Such structures have limited spatial and temporal extent. The streaks that appear in the boundary layer of channel flow are an example. The overall accuracy of the flow computation is sacrificed if the grid resolution is not fine enough to capture the streaks. Extending the fine grid required to resolve wall streaks to the entire domain is prohibitively expensive. The situation bears some resemblance to those in which AMR has been applied with success.

There is however a significant difference between standard AMR applications and turbulent flow. In standard AMR the computational grids are set up quite frequently, every few time steps. The standard technique used to identify regions in which additional resolution is required is to compare predictions on a coarser and finer grid and use Richardson extrapolation to estimate whether the local truncation error is within acceptable limits. This implicitly assumes that the finest grids in the computation can achieve enough resolution so that the asymptotic error estimates based upon the formal order of accuracy of the numerical method are valid. In the context of turbulence computations this is equivalent to stating that the finest grids can achieve DNS-like resolution. This is prohibitive and a modification of AMR to account for unresolved scales of motion is necessary.

Previous work has also sought to address the problem of differentiating between scales that should be resolved and others that can be economically modeled. An early idea due to Voke [18] was to use multiple meshes as a tool in accelerating convergence to a quasi-steady state. The Dynamic Multilevel (DML) method of Dubois, Jauberteau and Temam [7] can be seen as an alternative to LES. Instead of modeling subgrid stresses using a physical model, in DML the small scales are computed less accurately using lower-order schemes with larger time steps. Terra-

col, Sagaut and Basdevant [16] have suggested freezing the small scales
while a number of time steps are taken on the coarser grids. In order not
to lose small-scale dynamics, they suggest a periodic prolongation of the
large-scale velocity fields using small-scales stored from previous time
steps. Both the large and small scales are advanced in time for a few
steps after which a new large scale velocity field is obtained by filtering.
This procedure raises the question of the equilibrium between small and
large scales during the prolongation stage. This step of the algorithm
might effectively act as an external, non-physical excitation. Quémére,
Saguat and Couaillier [15] presented a procedure in which patched grids
of different resolutions were used in a channel flow. They show that
considerable economy may be obtained by using fine grids only in the
wall region but also remark that numerical artefacts arose at the grid
boundaries.

1.2   Governing equations

The governing equations are the filtered, compressible Navier-Stokes
equations for an ideal gas

$$\frac{\partial \bar{U}}{\partial t} + \frac{\partial \bar{F}_1}{\partial x_1} + \frac{\partial \bar{F}_2}{\partial x_2} + \frac{\partial \bar{F}_3}{\partial x_3} = 0,$$

$$\bar{U} = \begin{bmatrix} \bar{\rho} & \bar{\rho}\tilde{u}_1 & \bar{\rho}\tilde{u}_2 & \bar{\rho}\tilde{u}_3 & \bar{\rho}\tilde{e} \end{bmatrix}^T,$$

$$\bar{F}_i = \begin{bmatrix} \bar{\rho}\tilde{u}_i \\ \bar{\rho}\tilde{u}_i\tilde{u}_1 + \bar{p}\delta_{i1} - \tau_{i1} - \mu\tilde{S}_{i1} \\ \bar{\rho}\tilde{u}_i\tilde{u}_2 + \bar{p}\delta_{i2} - \tau_{i2} - \mu\tilde{S}_{i2} \\ \bar{\rho}\tilde{u}_i\tilde{u}_3 + \bar{p}\delta_{i3} - \tau_{i3} - \mu\tilde{S}_{i3} \\ (\bar{\rho}\tilde{e} + \bar{p})\tilde{u}_i - Q_i - \mu\tilde{S}_{ij}\tilde{u}_j - k\dfrac{\partial \theta}{\partial x_i} \end{bmatrix},$$

with $^-$ denoting grid filtering, and $^\sim$ density-weighted averaging. The
filtered equation of state is $\bar{p} = \bar{\rho}R\tilde{T}$, the diagonal term of the subgrid-
stress tensor is neglected [8], the resolved energy is

$$\bar{\rho}\tilde{e} = \bar{\rho}c_v T + \frac{1}{2}\bar{\rho}\left(\tilde{u}_1^2 + \tilde{u}_3^2 + \tilde{u}_3^2\right),$$

the Sutherland relation for constant Prandtl $\mathrm{Pr} = c_p\mu(\theta)/k(\theta) = 0.7$ is
applied, and the system is closed with variable density eddy-viscosity
and diffusivity models

$$\tau_{ij} = \bar{\rho}\nu_t\tilde{S}_{ij}, \quad Q_i = \bar{\rho}\frac{\nu_t}{\mathrm{Pr}_t}\frac{\partial \theta}{\partial x_i}.$$

1.3   Filtering procedures

The general multi-level filtering framework proposed by Germano [9] is adopted. Each grid level has an associated filter operation G_n. Filters from the same family (i.e. top hat in the applications presented here) are used at all levels. Filtered variables may be defined at each grid level by $\langle \phi \rangle_n (\mathbf{x}, t) = (G_n * \phi)(\mathbf{x}, t)$. The coarsest grid level is denoted by 0 and the finest existent at a given space-time locale by L. The Navier-Stokes equations from above, $\partial_t U + N(U) = 0$ become

$$\partial_t \langle U \rangle_n + N(\langle U \rangle_n) = -T_n$$

after filtering. The closure procedure parallels that presented for a single filtering operation in the previous section.

1.4   Flow feature diagnostics

Standard AMR is typically viewed as a black box that may applied to the solution of any time varying problem that exhibits localized features. The criterion governing grid refinement is mathematical in nature and typically does not include any physical knowledge about the particular problem being solved. On the other hand, most multi-level techniques that have been proposed for turbulence simulation rely heavily upon physical modeling of the subgrid scale effects. For instance, in DML [7] the freezing of the small scales when taking coarse grid time steps is justified by the different characteristic times in which small and larger scale turbulence achieves local equilibrium. The point of view espoused in this paper is that probably both ingredients are required in order to achieve a successful algorithm. The particular method studied here is a combination of *a posteriori* error analysis combined with physical analysis.

Initially the standard technique of error estimation based upon Richardson extrapolation [5] was tried. This was unsatisfactory as it led to a rapid increase in the overall number of points. A resolution typical of DNS was set up by this procedure. The approach that was successful consists of a combination of error estimation and physical reasoning. Recently, Adjerid et al. [1] have analyzed the error of a class of discontinuous Galerkin methods applied to hyperbolic problems that include the standard finite volume schemes typically used in compressible fluid computations. Essentially, the procedure recognizes that for a given polynomial approximation of the solution of degree p over an element of extent h, the discretization error is generally $O(h^{p+1})$. At certain points within the element, that correspond to the roots of the difference of two Legendre polynomials, the error is $O(h^{p+2})$. For details the reader is

directed to [1]. The different spatial orders of accuracy permit a rapid *a posteriori* estimate of the accuracy achieved on the cells at any one particular grid level. Rather than obtaining the error estimate by comparison to a test integrating in time on a coarser grid, only the results from a trial time step on the current grid level is required.

Changing the mathematical error estimation method is not enough. Tests using the *a posteriori* error estimate again led to excessive refinement and consequent loss of economy of computation. An examination of the flow field showed that this occurred even in regions where the fluid turbulence was essentially isotropic and suitable for modeling by the subgrid scale terms. A physical correction of the error estimator was therefore added. In the regions flagged for refinement by the error estimator two physical indicators were computed: the enstrophy $|\nabla \times \vec{u}|$ and the scalar product of the local velocity and vorticity $|(\nabla \times \vec{u}) \cdot \vec{u}|$. Only when one of the physical indicators exceeded a threshold value was the region subject to refinement. In effect the physical indicators act to discriminate interesting dynamics that includes prominent vortex tubes from that of locally near-isotropic turbulence. The cutoff value was determined by numerical experimentation. This is unsatisfactory and further analysis is underway to establish a more rational procedure of establishing a cutoff value. Other indicators suggested by coherent structure eduction procedures are also undergoing tests.

1.5   Communication between grids

An important aspect in a multilevel algorithm is to establish procedures for communication of data between grids on various levels. This involves two operations: (1) a prolongation operation P from coarse to fine grids and; (2) a restriction operation R from fine to coarse grids. Standard AMR typically uses a linear interpolation to define P and a cell averaging procedure to define R. A modification of these procedures was found to be necessary in the context of applying AMR to LES. The prolongation operator is applied whenever new fine grids are generated. Generally there is significant overlap between the new fine grids and previously generated grids at the same level since coherent structures that require better resolution are advected with the mean flow. In order not to lose dynamic content (high frequency contributions), fine grids are first initialized to previously computed values at the same grid level in areas of grid overlap. The prolongation operator is only applied to newly created fine grids, at level l say, where no grids of level l existed previously. Straightforward linear interpolation was found to induce excessive subgrid cell excitation. This had the effect of increasing the

number iterations in the pseudo-time variable (see below) required to achieve convergence at a given physical time step. Faster convergence was achieved by using the truncation of the dispersion relation from the Navier-Stokes equations to the wavenumbers resolvable on the newly created grid. This relation was used to define the newly resolvable spectral content by assuming that the energy spectrum follows a power law. The power law coefficient was taken to depend on the region of the spectrum, i.e. a quadratic interpolation of the power law coefficient from $m = 4$ in the energy containing eddy region to $m = -5/3$ in the inertial range.

A number of previous multi-level turbulence simulations (e.g. [15]) mentioned difficulties at the boundaries between coarse and fine grids due to the effect of averaging. Simple averaging was found to have the same effect in the computations carried out here. However, conservative fix-ups [5], [4] in which the more accurately computed fluxes on fine grids are used to update adjoining coarse grid values was found to work well.

2.   Numerical Methods

2.1   Unstructured Grid Algorithm

The unstructured grid algorithm uses an embedded tetrahedral grid approach implemented as an octal tree structure (OCTLES - Octal Tree Large Eddy Simulation code) [13]. There are several options for treating the convective terms from the Navier-Stokes equations. These include multi-dimensional fluctuation splitting [6], second order reconstruction and approximate Riemann solvers along the cell interface normal direction [17] and multi-dimensional wave propagation techniques [12]. The convective terms are advanced in time explicitly. Diffusive terms are treated implicitly. A pseudo-time stepping technique [3] is used within each physical time step to solve the resulting implicit system. Subgrid-scale turbulent stresses are included using the dynamic model [10]. An interesting feature of this application of the dynamic model is that subgrid-scale stresses are computed for each grid pair between the coarsest, initial grid and the finest grid present. This has been observed to speed up the convergence of the pseudo-time iterations required to determine the contribution of the viscous terms. The code has been validated [14] by comparison to a number of test cases proposed in [2]. Grid adaptation is carried out by recursive subdivision of an initial tetrahedral grid.

2.2   Structured Cartesian grid algorithm

An alternative to the complicated program structures required for unstructured girds is to use embedded Cartesian grids [5]. The grid generation procedures are much simpler in this case, but the problem of boundary representation appears for general geometries. In order to test the AMR-LES procedures, sample computations have been performed only in a rectangular geometry. The computer code for this approach (BEARCLAW -Boundary Embedded Adaptive Refinement Conservation Law) allows for a number of treatments of the convective and source terms. These parallel those presented in the unstructured grid case. The BEARCLAW code may be freely downloaded from www.washington.edu/~claw.

3.   Applications

3.1   Stationary and rotational channel flow

The above procedures are now tested on channel flow. Both a stationary channel and one rotating along an axis in the spanwise mean flow direction are considered. The AMR-LES results are compared to DNS results [11]. The half channel width, bulk velocity Reynolds number is $Re = U_b h/\nu = 2900$. The rotating channel has a Rossby number $Ro = 2\Omega h/U_b = 0.5$. The second order wave propagation algorithms of [12] are used to treat the convective terms in both the structured and unstructured computations presented here. A comparison between the DNS results and those obtained by the two AMR methods is presented in fig. 1-2 for the turbulent stress. An initial, coarsest level, grid of dimensions $32x32x32$ was used. A tetrahedral grid was obtained by splitting each hexahedron of the regular Cartesian grid in six tetrahedra. The AMR results are within 1% of the DNS results for the stationary channel flow. Both the structured and unstructured methods perform similarly on this case. This is thought to result from the overall symmetry of the flow and the fact that the tetrahedral grid was obtained by destructuring the Cartesian grid. It is apparent from fig. 1 that the AMR algorithms place finer resolution in the high shear regions closer to the walls. When rotation is applied the AMR-LES methods exhibit lower accuracy. The maximum error observed in the turbulent stress was 2.4%. Also, the loss of symmetry imposed by the rotation led to different grid placement in the unstructured algorithm with respect to the Cartesian algorithm. Higher error levels were observed for the tetrahedral grid algorithm. Instantaneous vorticity plots of the flow computed by the Cartesian AMR-LES method are presented in fig. 3-4. It may

be observed that the AMR procedure captures the rich dynamics of the near-wall region and the relaminarization which occurs on the rotating channel suction side.

4.   Conclusions

An adaptive mesh refinement methodology for large eddy simulation has been proposed. LES in itself reduces the dynamic complexity of simulating fluid turbulence. It is asserted that adaptive refinement may offer further reductions of the degrees of freedom that need to be resolved. The AMR-LES algorithm proposed here differs from standard AMR algorithms. There are always some dynamics taking place at the unresolved scale, so the usual error estimation procedures used to add mesh points do not carry over directly. Rather, a combined strategy incorporating both numerical estimates and physical flow features is applied. The overall effect is to employ greater grid resolution in regions in which the subgrid effects relative to grid level l are diagnosed as involving significant deviations from isotropic turbulence. In regions in which the indicator suggests that subgrid fluctuations are isotropic in nature, a standard dynamic, eddy-viscosity model is used to provide closure terms. Full testing of the method is still in progress and shall be reported at a later date.

Acknowledgments

References

[1] S. Adjerid, L. Krivodonova, J. Flaherty, and K. Devine. An a posteriori error estimate for the discontinuous galerkin method for hyperbolic problems. *Comp. Meth. Appl. Mech. Engrng.*, (to appear).

[2] AGARD. A selection of test cases for the validation of large-eddy simulations of turbulent flows. Technical Report 345, AGARD, 1998.

[3] A. Arnone, M.-S. Liou, and L. Povinelli. Integration of Navier-Stokes equations using dual time stepping and a multigrid method. *AIAA J.*, 33:985–990, 1995.

[4] M. Berger and R. LeVeque. Adaptive mesh refinement using wave-propagation algorithms for hyperbolic systems. *SIAM J. Num. Analysis*, 35:2298–2316, 1998.

[5] M. J. Berger and J. Oliger. Adaptive mesh refinement for hyperbolic partial differential equations. *J. Comp. Phys.*, 53:484–512, 1984.

[6] H. Deconinck, R. Struijs, H. Bourgois, H. Paillere, and P. Roe. Multidimensional upwind methods for compressible flows. *AGARD*, R-787, 1992.

[7] T. Dubois, F. Jauberteau, and R. Temam. *Dynamic Multilevel Methods and the Numerical Simulation of Turbulence*. Cambridge University Press, Cambridge, 1999.

[8] G. Erlebacher, M. Hussaini, C. Speziale, and T. Zang. Toward the large-eddy simulation of CompressibleTurbulent flows. *J. Fluid Mech.*, 238:155–185, 1992.

[9] M. Germano. Turbulence: the filtering approach. *J. Fluid Mech.*, 238:325–336, 1992.

[10] M. Germano, U. Piomelli, P. Moin, and W. Cabot. A dynamic subgrid-scale eddy viscosity model. *Phys. Fluids*, A 3:1760, 1991.

[11] R. Kristoffersen and H. Andersson. Direct simulations of low-reynolds-number turbulent flow in a rotating channel. *J. Fluid Mech.*, 256:163–197, 1993.

[12] R. LeVeque. Wave propagation algorithms for multidimensional hyperbolic systems. *J. Comp. Phys.*, 131:327–353, 1997.

[13] S. Mitran, D. Caraeni, and D. Livescu. Large eddy simulation of unsteady rotor-stator interaction in a centrifugal compressor. In *33rd*

AIAA/ASME/SAE/ASEE Joint Propulsion Conference and Exhibit, New York, 1997. AIAA.

[14] S. Mitran and P. Cizmas. LES calibration of a turbulent potential model for turbomachinery flows. In *AIAA/ASME/SAE/ASEE Joint Propulsion Conference and Exhibit*. AIAA Paper 2000-3203, 2000.

[15] P. Quémêré, P. Sagaut, and V. Couailler. Une méthode multido-maine/multirésolution avec application à la simulation des grandes échelle. *Comptes rendus de l'Académie des sciences - Série IIb - Mécanique*, 328:87–90, 2000.

[16] M. Terracol, P. Sagaut, and C. Basdevant. A multilevel / multiresolution approach for large-eddy simulation. In *European Congree on Computational Methods in Applied Sciences and Engineering (ECCOMAS 2000)*, 2000.

[17] V. Venkatakrishnan. Perspective on unstructured grid flow solvers. *AIAA J.*, 34:533–547, 1996.

[18] P. Voke. Multiple mesh simulation of turbulent flow. Technical Report QMW EP-1082, Queen Mary and Westfield College, University of London, 1990.
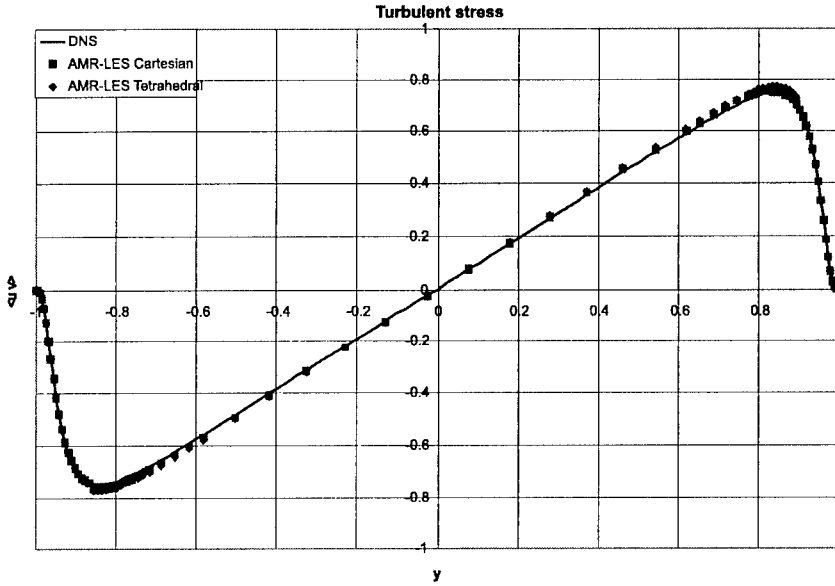
Figure 1. Comparison between DNS computation (line)[11], Cartesian grid AMR (squares) and tetrahedral grid AMR (diamonds). The turbulent stress along the channel span. Notice the larger grid spacing close the channel centerline and the smaller grid spacing near the walls.
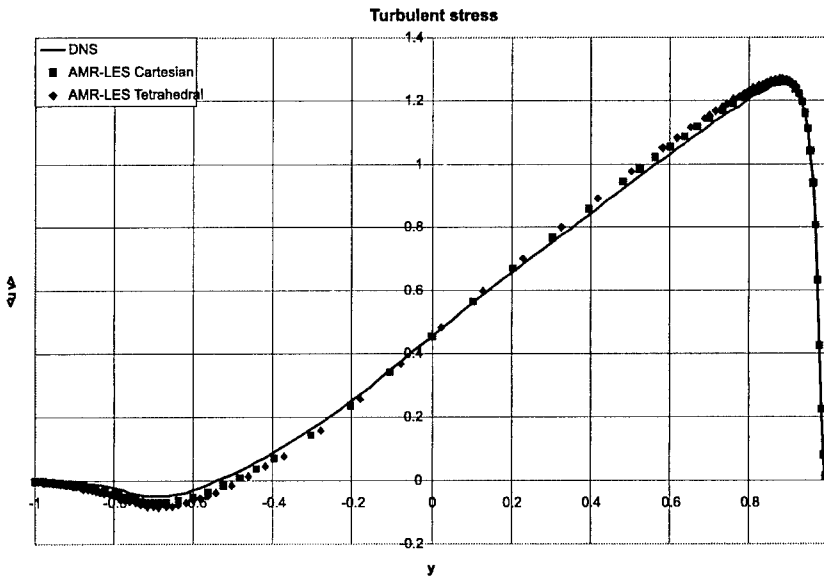
Figure 2. Similar to previous figure but for rotating channel, $Ro = 0.5$.
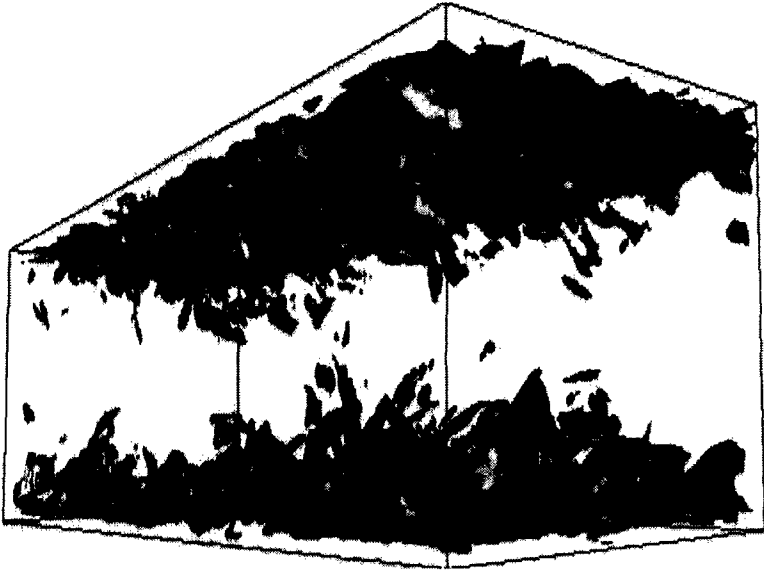
Figure 3.   Isovorticity surfaces computed using Cartesian AMR, stationary channel.
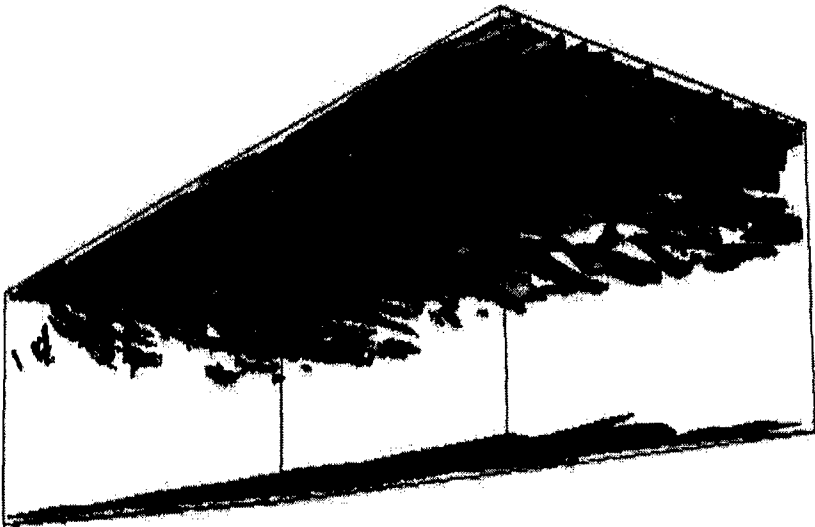
Figure 4.   Isovorticity surfaces computed using Cartesian AMR, rotating channel
$Ro = 0.5$.